

Nickel complexes supported by quinoline-based ligands: synthesis, characterization and catalysis in the cross-coupling of arylzinc reagents and aryl chlorides or aryltrimethylammonium salts†

Qiang Zhang, Xue-Qi Zhang and Zhong-Xia Wang*

Received 24th April 2012, Accepted 8th June 2012

DOI: 10.1039/c2dt30886j

Lithium and nickel complexes bearing quinoline-based ligands have been synthesized and characterized. Reaction of 8-azidoquinoline with Ph_2PNHR ($\text{R} = p\text{-MeC}_6\text{H}_4$, Bu^t) affords *N*-(8-quinolyl)-iminophosphoranes $\text{RNHP}(\text{Ph}_2)=\text{N}(8\text{-C}_9\text{H}_6\text{N})$ (**1a**, $\text{R} = p\text{-MeC}_6\text{H}_4$; **1b**, $\text{R} = \text{Bu}^t$, $\text{C}_9\text{H}_6\text{N} = \text{quinolyl}$). Reaction of **1a** with $(\text{DME})\text{NiCl}_2$ generates a nickel complex $[\text{NiCl}_2\{\text{N}(8\text{-C}_9\text{H}_6\text{N})=\text{P}(\text{Ph}_2)\text{NH}(p\text{-MeC}_6\text{H}_4)\}]$ (**2a**). Treatment of **1b** with $(\text{DME})\text{NiCl}_2$ and following with NaH produces $[\text{NiCl}\{(1,2\text{-C}_6\text{H}_4)\text{P}(\text{Ph})(\text{NHBu}^t)=\text{N}(8\text{-C}_9\text{H}_6\text{N})\}]$ (**4**). Complex **4** was also obtained by reaction of $(\text{DME})\text{NiCl}_2$ with $[\text{Li}\{(1,2\text{-C}_6\text{H}_4)\text{P}(\text{Ph})(\text{NHBu}^t)=\text{N}(8\text{-C}_9\text{H}_6\text{N})\}]$ (**5**) prepared through lithiation of **1b**. Reaction of 2-Py $\text{CH}_2\text{P}(\text{Ph}_2)=\text{N}(8\text{-C}_9\text{H}_6\text{N})$ (**6**, Py = pyridyl) and $\text{PhN}=\text{C}(\text{Ph})\text{CH}_2\text{P}(\text{Ph}_2)=\text{N}(8\text{-C}_9\text{H}_6\text{N})$ (**8**), respectively, with $(\text{DME})\text{NiCl}_2$ yields two five-coordinate *N,N,N*-chelate nickel complexes, $[\text{NiCl}_2\{2\text{-PyCH}_2\text{P}(\text{Ph}_2)=\text{N}(8\text{-C}_9\text{H}_6\text{N})\}]$ (**7**) and $[\text{NiCl}_2\{\text{PhN}=\text{C}(\text{Ph})\text{CH}_2\text{P}(\text{Ph}_2)=\text{N}(8\text{-C}_9\text{H}_6\text{N})\}]$ (**9**). Similar reaction between $\text{Ph}_2\text{PCH}_2\text{P}(\text{Ph}_2)=\text{N}(8\text{-C}_9\text{H}_6\text{N})$ (**10**) and $(\text{DME})\text{NiCl}_2$ results in five-coordinate *N,N,P*-chelate nickel complex $[\text{NiCl}_2\{\text{Ph}_2\text{PCH}_2\text{P}(\text{Ph}_2)=\text{N}(8\text{-C}_9\text{H}_6\text{N})\}]$ (**11**). Treatment of $[(8\text{-C}_9\text{H}_6\text{N})\text{N}=\text{P}(\text{Ph}_2)_2\text{CH}_2]$ (**12**) [prepared from $(\text{Ph}_2\text{P})_2\text{CH}_2$ and 2 equiv. of 8-azidoquinoline] with LiBu^n and $(\text{DME})\text{NiCl}_2$ successively affords $[\text{NiCl}\{(8\text{-C}_9\text{H}_6\text{N})\text{NP}(\text{Ph}_2)_2\text{CH}\}]$ (**13**). The new compounds were characterized by ^1H , ^{13}C and ^{31}P NMR spectroscopy (for the diamagnetic compounds), IR spectroscopy (for the nickel complexes) and elemental analysis. Complexes **2a**, **4**, **7**, **9**, **11** and **13** were also characterized by single-crystal X-ray diffraction techniques. The nickel complexes were evaluated for the catalysis in the cross-coupling reactions of arylzinc reagents with aryl chlorides and aryltrimethylammonium salts. Complex **7** exhibits the highest activity among the complexes in catalyzing the reactions of arylzinc reagents with either aryl chlorides or aryltrimethylammonium bromides.

Introduction

Transition-metal-catalyzed cross-coupling reactions, including Kumada, Negishi, Suzuki, Stille and Hiyama reaction, are reliable and versatile tools in modern organic synthesis.^{1,2} The Negishi reaction is one of the most useful methods for constructing new C–C bonds because of the ready availability and the functional-group compatibility of the organozinc reagents.^{1,3} Organic bromides and iodides are usually employed as the electrophilic substrates in the cross-coupling reactions.⁴ The use of organic chlorides as electrophiles has proven more difficult due to low reactivity of the C–Cl bond. However, chlorides are more useful substrates due to their lower cost and the wider diversity

of available compounds.⁵ Hence the catalytic coupling reactions using organic chlorides as electrophiles have attracted intensive attention in the past decade. The Negishi reaction using chlorides as the electrophiles has also achieved important progress. For example, Herrmann and co-workers reported the first example of a palladium-catalyzed Negishi coupling of an unactivated aryl chloride in 1999.⁶ Dai and Fu reported the first general method for palladium-catalyzed Negishi cross-coupling of aryl chlorides in 2001.^{5a} Milne and Buchwald found an extremely active palladium catalyst for the coupling reaction of aryl chlorides.⁷ Organ and co-workers found that NHC-coordinated palladium complexes (Pd-PEPPSI) can catalyze aryl–aryl and alkyl–alkyl coupling of organozinc reagents and chlorides.⁸ However, inexpensive nickel-based catalysts are less successful for the coupling reaction of unactivated chlorides with organozinc reagents although a few examples have been reported.^{9–11} Development of highly active and widely applicable nickel catalysts for the cross-coupling of chloride substrates is still of significance.

On the other hand, nitrogen-containing compounds such as alkyl- and arylamines are potential electrophiles in catalytic

CAS Key Laboratory of Soft Matter Chemistry and Department of Chemistry, University of Science and Technology of China, Hefei, Anhui 230026, People's Republic of China. E-mail: zzwang@ustc.edu.cn; Fax: +86 551 3601592; Tel: +86 551 3603043

† Electronic supplementary information (ESI) available: ESR and UV spectra of complexes **2a**, **7**, **9**, **11** and **13**. CCDC reference numbers 878348–878353. For ESI and crystallographic data in CIF or other electronic format see DOI: 10.1039/c2dt30886j

cross-couplings because these compounds are widely available in the natural world and in industry. The amino groups in arylamines are also important activating and directing groups which can lead to selective functionalization of aromatic rings. However, cross-coupling reactions through C–N bond cleavage of arylamines are scarce. In 2007 Kakiuchi and co-workers reported a ruthenium-catalyzed Suzuki coupling through C–N bond cleavage of anilines, but a carbonyl group at the *ortho* position of the amino group is indispensable.¹² Several examples using aryltrimethylammonium salts as electrophilic substrates have been reported. Wenkert and co-workers carried out the nickel-catalyzed reaction of aryltrimethylammonium iodides with Grignard reagents in the early stage of cross-coupling studies. However, this method suffers from a limited substrate scope and low product yields.¹³ Recently, Reeves *et al.* developed the coupling using aryltrimethylammonium triflates as the electrophiles and $(\text{Ph}_3\text{P})_2\text{PdCl}_2$ as the catalyst.¹⁴ In 2003, Blakey and MacMillan carried out the Suzuki coupling of aryltrimethylammonium triflates with $\text{Ni}(\text{cod})_2/\text{IMes}$ as a catalyst.¹⁵ Our group performed the coupling of aryltrimethylammonium iodides and aryl or alkylzinc chlorides catalyzed by $(\text{C}_3\text{P})_2\text{NiCl}_2$, and more recently, by pincer nickel complexes.¹⁶

We intended to design new catalysts for improving the catalysis in the activation of C–Cl and C–N bonds. To achieve the aim, the choice of ligands is crucial because the properties of the complexes strongly rely on supporting ligands besides the metal itself. Our studies have shown that pincer nickel complexes (*e.g.* **I–IV** in Chart 1) are active in catalyzing cross-coupling of arylzinc reagents with aryl chlorides or aryltrimethylammonium salts.^{11a,b,16b} In complexes **II** and **III**, the *N*-heterocyclic carbene and the iminophosphoranyl nitrogen atom are strong electron-donor groups. Replacement of the carbene part with a weaker electron-donor group will tune the electron property of the central metal and make the side-arm coordinate group dissociation from the central metal easier, which will possibly change the catalytic behavior of these complexes. The quinolyl group seems a logical choice due to the modest electron-donor ability of its nitrogen atom. Quinoline-based complexes of transition metals also show good catalytic activity in C–C bond formation reactions.¹⁷ We also hoped to improve catalysis of complex **IV** in the cross-coupling of aryltrimethylammonium

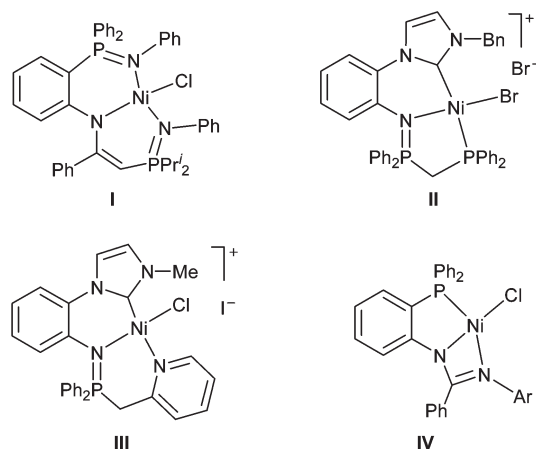


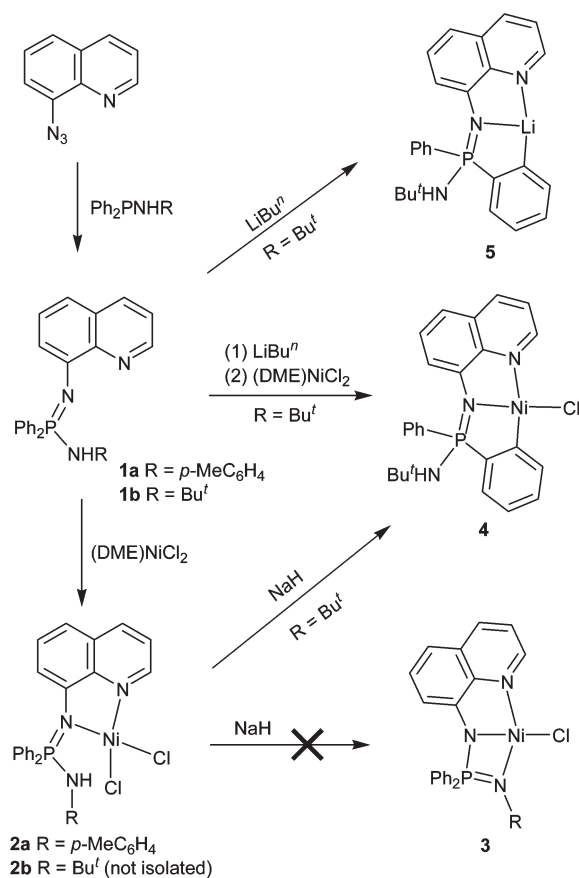
Chart 1

salts with arylzinc reagents through modification of the ligand by replacing the imino group in complex **IV** using an iminophosphoranyl group. Iminophosphoranes essentially behave as strong π and σ donor ligands and do not exhibit π accepting capacity in contrast to imines.¹⁸ These properties of iminophosphoranes in the ancillary ligands will provide different electronic environments at the metal center and hence regulate the catalytic properties of the complexes. Based on the ideas, we designed new ligands which involve quinolyl and iminophosphoranyl motifs, synthesized and characterized a series of nickel complexes bearing these ligands, and evaluated the catalysis of the nickel complexes in the reactions of aryl chlorides or aryltrimethylammonium salts with arylzinc chlorides. Here we report the results.

Results and discussion

Synthesis and characterization of ligands and complexes

Synthesis of ligands **1a**, **1b** and complexes **2a–5** are summarized in Scheme 1. Reaction of 8-azidoquinoline with Ph_2PNHR ($\text{R} = p\text{-MeC}_6\text{H}_4$, Bu^t) produces *N*-(8-quinolyl)iminophosphoranes $\text{RNHP}(\text{Ph})_2=\text{N}(8\text{-C}_9\text{H}_6\text{N})$ (**1a**, $\text{R} = p\text{-MeC}_6\text{H}_4$; **1b**, $\text{R} = \text{Bu}^t$). Reaction of **1a** with $(\text{DME})\text{NiCl}_2$ gives a *N,N*-chelate nickel complex $[\text{NiCl}_2\{\text{N}(8\text{-C}_9\text{H}_6\text{N})=\text{P}(\text{Ph})_2\text{NH}(p\text{-MeC}_6\text{H}_4)\}]$ (**2a**). Treatment of **1b** with $(\text{DME})\text{NiCl}_2$ and following with NaH forms $[\text{NiCl}\{(1,2\text{-C}_6\text{H}_4)\text{P}(\text{Ph})(\text{NHBu}^t)=\text{N}(8\text{-C}_9\text{H}_6\text{N})\}]$ (**4**),

Scheme 1 Synthesis of compounds **1a–5**.

rather than *N,N,N*-chelate nickel complex **3**. The first step of the reaction should give a *N,N*-chelate nickel complex **2b**. Treatment of **2b** with NaH leads to deprotonation of one of the phenyl groups attached on the phosphorus atom of complex **2b** and formation of a C–Ni bond. Construction of the Ni–N=P–N four-membered ring in **3** through deprotonation of the NH to be difficult and instead, a deprotonation process on the phenyl group proceeded. Complex **4** was also obtained by reaction of **1b** with LiBuⁿ and then treatment with (DME)NiCl₂. In this reaction LiBuⁿ abstracts a proton from the phenyl group rather than NH group attached on the phosphorus atom, forming *N,N*, *C*-chelate lithium complex [Li{(1,2-*C*₆H₄)P(Ph)(NHBu^t)=N-(8-*C*₉H₆N)}] (**5**). Attempts to transform **2a** into **3** or an analogue of **4** by treatment with NaH were unsuccessful, the reaction leading to an unidentified mixture. Both **1a** and **1b** are crystalline solids and gave satisfactory elemental analytical results. Their structures were also confirmed by ¹H, ¹³C and ³¹P NMR spectroscopy. Complex **2b** was not isolated and was directly applied for further reactions.

Complex **2a** is a paramagnetic crystalline solid which gave satisfactory elemental analysis. Its IR spectrum displays a NH absorption at 3222 cm⁻¹. Single-crystal X-ray diffraction (Fig. 1) shows that the quinolyl nitrogen atom (N1) and the iminophosphoranyl nitrogen atom (N2) of the ligand coordinate to the central nickel atom, while the amino nitrogen atom (N3) is coordination-free. The four-coordinated nickel atom has a distorted tetrahedral coordination geometry and is coplanar with the N1C5C6N2 plane. The Ni–N1 distance of 1.981(4) Å is slightly longer than the corresponding value in *P,N*(quinolyl)-chelate nickel complex Ni[8-{Ph(Me)P}C₉H₆N]^{2,19} but comparable to that of Ni–N1 in [NiBr₂{(*o*-Pr^tOC₆H₄)N=C(SiMe₃)CH₂(2-Py)}] [1.986(3) Å]. The Ni–N2 distance of 1.996(3) Å are

close to that of Ni–N2 in [NiBr₂{(*o*-Pr^tOC₆H₄)N=C(SiMe₃)CH₂(2-Py)}] [1.993(3) Å].²⁰ The P1–N2 distance of 1.601(3) Å is a little longer than a P–N double bond which is about 1.57 Å, and the P1–N3 distance of 1.641(4) Å is between a formal P–N single (1.77 Å) and double bond.²¹

Complex **4** is a deep red diamagnetic crystalline solid which was characterized by elemental analysis, ¹H, ¹³C and ³¹P NMR and IR spectroscopy. Both ¹H NMR and IR spectra show the presence of an NH group. For example, its ¹H NMR spectrum exhibits a NH signal at δ 3.19 ppm as a doublet. The IR spectrum displays the NH absorption at 3198 cm⁻¹. The structure was further confirmed by single-crystal X-ray diffraction (Fig. 2). In the complex the central nickel atom is surrounded by the quinolyl nitrogen atom (N1), the iminophosphoranyl nitrogen atom (N2), the carbon atom (C11) of the phenylene and a chlorine atom, having a distorted square-planar coordination geometry. The phosphorus atom is also approximately coplanar with the plane constituted by N1N2C11C11Ni1 atoms. Both N1–Ni–C11 and N2–Ni–C11 are approximately linear, the bond angles being 171.69(14) and 176.69(9)°, respectively. The amido nitrogen atom is sp² hybridized, the sum of the angles around N2 being 359.99°. The Ni–N1 distance of 1.961(3) Å is shorter than those of Ni–N1 in complex **2a** and Ni–N(Py) in the complex [Ni(Cl){2-(CN(Me)-(CH₂)₂-N)C₆H₄N=P(Ph₂)CH₂Py}]⁺I⁻ [1.984(4) Å],^{11b} but within a normal range. The Ni–N2 distance of 1.891(2) Å is very close to the corresponding bond in an amido pincer nickel complex [Ni-(Cl){N{CH(Ph)P(Ph₂)=O}C₆H₄(PPh₂)-2}] [1.893(5) Å].²² The Ni–C11 distance of 1.885(3) Å is comparable to the C–Ni bond lengths in arylnickel complexes.²³ The P1–N2 distance of 1.608(3) Å is a little longer than a typical P–N double bond (1.57 Å), while the P1–N3 distance of 1.631(2) Å is between a formal P–N single and double bond.²¹

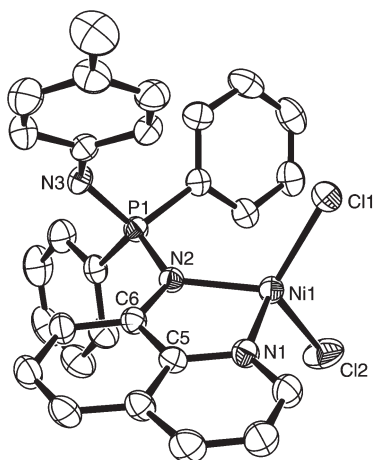


Fig. 1 ORTEP drawing of complex **2a** (30% probability; CH₂Cl₂ molecule is omitted). Selected bond lengths (Å) and angles (°): Ni(1)–N(1) 1.981(4), Ni(1)–N(2) 1.996(3), Ni(1)–Cl(1) 2.2154(14), Ni(1)–Cl(2) 2.2294(15), P(1)–N(2) 1.601(3), P(1)–N(3) 1.641(4), N(1)–C(5) 1.383(5), N(2)–C(6) 1.413(5); N(1)–Ni(1)–N(2) 83.30(15), N(1)–Ni(1)–Cl(1) 111.67(12), N(2)–Ni(1)–Cl(1) 115.24(10), N(1)–Ni(1)–Cl(2) 105.39(11), N(2)–Ni(1)–Cl(2) 117.89(11), Cl(1)–Ni(1)–Cl(2) 117.23(6), C(5)–N(1)–Ni(1) 113.1(3), C(6)–N(2)–Ni(1) 111.4(3), N(2)–P(1)–N(3) 113.87(19).

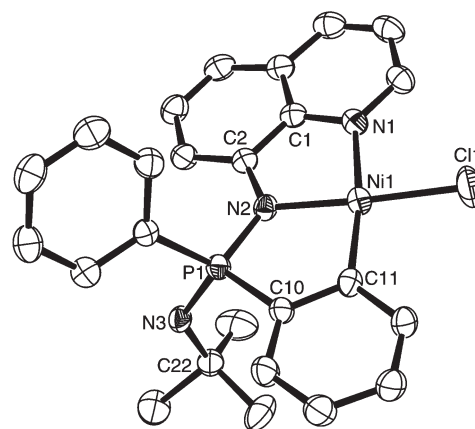
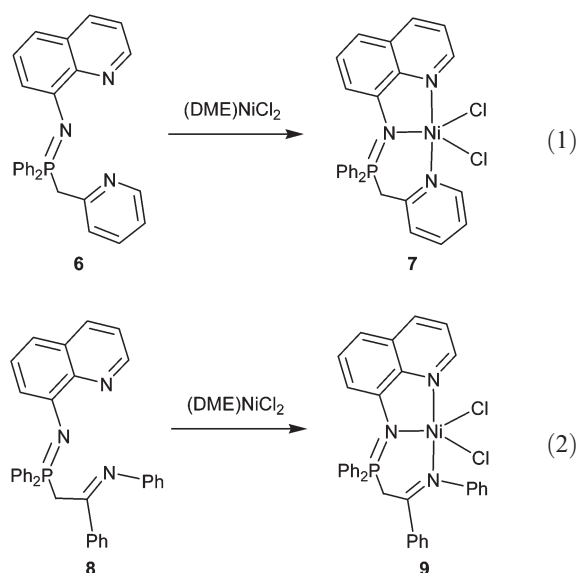


Fig. 2 ORTEP drawing of complex **4** (30% probability; THF molecule is omitted). Selected bond lengths (Å) and angles (°): Ni(1)–N(1) 1.961(3), Ni(1)–N(2) 1.891(2), Ni(1)–C(11) 1.885(3), Ni(1)–Cl(1) 2.1695(11), N(2)–P(1) 1.608(3), N(3)–P(1) 1.631(2), N(3)–C(22) 1.486(4), P(1)–C(10) 1.765(3), N(2)–C(2) 1.390(4); C(11)–Ni(1)–N(2) 88.18(13), C(11)–Ni(1)–N(1) 171.69(14), N(2)–Ni(1)–N(1) 83.51(12), C(11)–Ni(1)–Cl(1) 94.96(11), N(2)–Ni(1)–Cl(1) 176.69(9), N(1)–Ni(1)–Cl(1) 93.34(9), C(1)–N(1)–Ni(1) 112.1(2), C(2)–N(2)–P(1) 125.8(2), C(2)–N(2)–Ni(1) 114.4(2), P(1)–N(2)–Ni(1) 119.79(14), C(10)–C(11)–Ni(1) 117.8(3), N(2)–P(1)–N(3) 120.52(13).

Complex **5** is a yellow crystalline solid and was characterized by elemental analysis and multinuclear NMR spectroscopy. Elemental analytical results match the expected C, H and N composition of complex **5**. The ^1H NMR spectrum indicates the presence of an NH signal at δ 3.56 ppm as a doublet and corresponding signals of other groups. The ^{13}C and ^{31}P NMR spectra are also consistent with the structure. In addition, elemental analysis and NMR spectra also show no coordinated solvent in the molecule. Hence the complex may be a dimer. Attempts to grow single crystals for X-ray diffraction analysis were unsuccessful.

The synthesis of complexes **7** and **9** is shown in eqn (1) and (2), respectively.



Treatment of $(\text{DME})\text{NiCl}_2$ with **6** in CH_2Cl_2 at room temperature generates complex **7** as yellow green crystals. Complex **9**, a red–orange crystalline solid, was prepared similarly by reaction of $(\text{DME})\text{NiCl}_2$ with **8** in CH_2Cl_2 . Both **7** and **9** are paramagnetic and were characterized by elemental analysis and IR spectroscopy. The structures were also further confirmed by single-crystal X-ray diffraction techniques. The ORTEP drawing of complex **7** is shown in Fig. 3, along with selected bond lengths and angles. The central nickel atom is five-coordinate and has a distorted square-pyramidal geometry. The Cl1N1N2N3 atoms as the base of the square pyramid are coplanar, the torsion angle being 0.3° with the nickel atom deviating a little from the plane. The metal ring consisting of Ni1N2P1C22C23N3 atoms adopts a boat-like conformation; the N2N3C23P1 atoms are approximately coplanar. The Ni–N1 distance of 2.0796(19) Å is close to that of Ni–N2 [2.0753(19) Å], and both of them are shorter than that of Ni–N3 which is 2.153(2) Å. These bond distances are within the normal range for a coordinated nickel complex.²⁴ It is also noted that the Ni–N1 distance in complex **7** is longer than the Ni–N(quinoly1) distance in complex **4**. This may be caused by different coordination numbers of the complexes. The P–N2 distance of 1.605(2) Å is almost the same as the corresponding distance in complex **4**, and is normal for a coordinated iminophosphorane.^{11b,22}

The structure of complex **9** is shown in Fig. 4, along with selected bond lengths and angles. The structure is similar to that

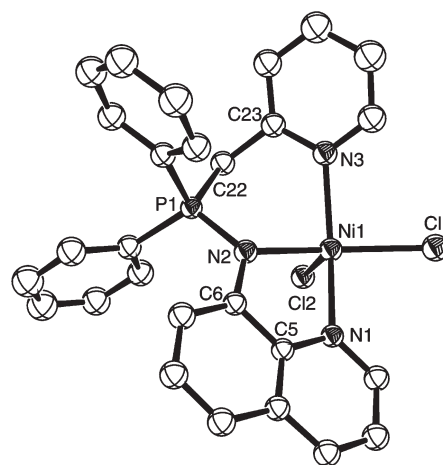


Fig. 3 ORTEP drawing of complex **7** (30% probability). Selected bond lengths (Å) and angles ($^\circ$): Ni(1)–N(1) 2.0796(19), Ni(1)–N(2) 2.0753(19), Ni(1)–N(3) 2.153(2), Ni(1)–Cl(1) 2.3403(8), Ni(1)–Cl(2) 2.3260(8), P(1)–N(2) 1.605(2), P(1)–C(22) 1.792(2), N(2)–C(6) 1.396(3), C(22)–C(23) 1.492(4); N(1)–Ni(1)–N(2) 78.82(7), N(2)–Ni(1)–N(3) 89.51(8), N(1)–Ni(1)–N(3) 157.53(8), N(2)–Ni(1)–Cl(2) 99.48(6), N(1)–Ni(1)–Cl(2) 99.20(6), N(3)–Ni(1)–Cl(2) 101.64(6), N(2)–Ni(1)–Cl(1) 158.76(6), N(1)–Ni(1)–Cl(1) 92.15(6), N(3)–Ni(1)–Cl(1) 92.06(6), Cl(1)–Ni(1)–Cl(2) 100.94(3), N(2)–P(1)–C(22) 106.38(11), C(6)–N(2)–P(1) 121.58(17), C(6)–N(2)–Ni(1) 114.31(15), P(1)–N(2)–Ni(1) 122.84(11).

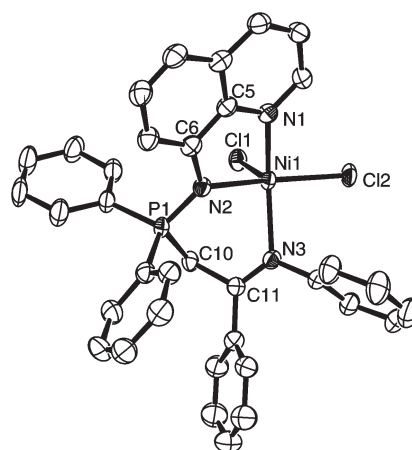


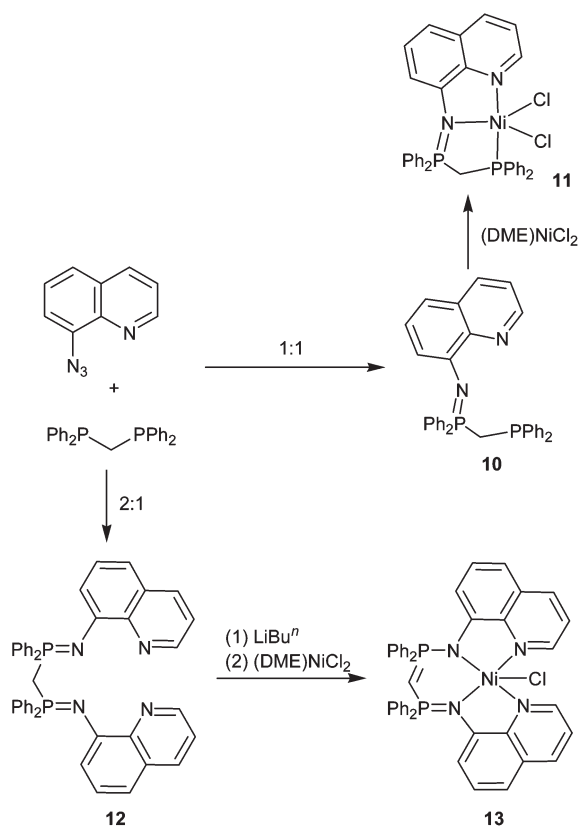
Fig. 4 ORTEP drawing of complex **9** (30% probability; THF and CH_2Cl_2 molecules are omitted). Selected bond lengths (Å) and angles ($^\circ$): Ni(1)–N(1) 2.052(6), Ni(1)–N(2) 2.052(5), Ni(1)–N(3) 2.171(6), Ni(1)–Cl(1) 2.328(2), Ni(1)–Cl(2) 2.296(2), N(2)–P(1) 1.602(6), P(1)–C(10) 1.806(7), C(10)–C(11) 1.523(9), N(3)–C(11) 1.264(9); N(1)–Ni(1)–Cl(1) 102.83(16), N(1)–Ni(1)–Cl(2) 94.59(19), N(2)–Ni(1)–Cl(1) 98.92(16), N(2)–Ni(1)–Cl(2) 164.76(16), N(3)–Ni(1)–Cl(1) 106.75(16), N(3)–Ni(1)–Cl(2) 91.29(17), N(1)–Ni(1)–N(2) 80.0(2), N(1)–Ni(1)–N(3) 149.0(2), N(2)–Ni(1)–N(3) 86.4(2), Cl(2)–Ni(1)–Cl(1) 96.18(7).

of complex **7**. Thus, the central nickel atom is five-coordinate and the coordination geometry is a very distorted square pyramid. However, unlike that of complex **7**, the base atoms of the square pyramid in complex **9** do not lie on a plane. The bond angle of N1NiN3 is $149.0(2)^\circ$ and the bond angle of N2NiCl2 is $164.76(16)^\circ$. The bond distances of both Ni–N1 and Ni–N2

[2.052(6) Å and 2.052(5) Å, respectively] are slightly shorter than the corresponding values in complex **7**, while the Ni–N3 distance of 2.171(6) Å is a little longer than the corresponding value in complex **7**. The P–N distance is close to that in complex **7**, and the C11–N3 distance of 1.264(9) Å is indicative of a C–N double bond.

The synthesis of compounds **11–13** is summarized in Scheme 2. Compound **10**, prepared from $(\text{Ph}_2\text{P})_2\text{CH}_2$ and an equimolar amount of 8-azidoquinoline, was treated with (DME)NiCl₂ to afford complex **11**. Reaction of $(\text{Ph}_2\text{P})_2\text{CH}_2$ with two equiv. of 8-azidoquinoline forms bis(iminophosphoranyl)methane **12**. Treatment of **12** with LiBu^n and following (DME)NiCl₂ yields complex **13**. Complex **11** is paramagnetic and was characterized by elemental analysis and IR spectroscopy. Single-crystal X-ray diffraction analysis confirms its molecular structure and the ORTEP drawing is displayed in Fig. 5. The central nickel atom is five-coordinate and has a distorted trigonal-bipyramidal geometry with the iminophosphorane nitrogen atom and two chlorine atoms occupying the equatorial positions and the quinolyl nitrogen atom and the phosphine atom occupying the axial positions. The N1NiP2 angle is 162.7(4)°, showing the atoms to be close to linear. The C11Cl12N2Ni atoms are coplanar, the sum of the angles at nickel being 360.0°. Due to poor data quality, the bond parameters are not further discussed.

Complex **13** is also a paramagnetic species and was characterized by elemental analysis, IR spectroscopy and single-crystal X-ray diffraction analysis. The ORTEP drawing is displayed in Fig. 6, along with selected bond lengths and angles.



Scheme 2 Synthesis of compounds **11–13**.

The five-coordinate nickel atom has a distorted trigonal-bipyramidal geometry. The N1 and N4 atoms occupy the axial positions and arrangement of N1NiN4 atoms is close to linear [bond angle = 170.52(14)°]. The N2N3C11 atoms occupy the equatorial positions and the N2N3C11Ni atoms are approximately coplanar, the sum of the angles at nickel being 359.50°. The metal ring consisting of P1C19P2N4Ni1N2 atoms adopts a boat-like conformation. The P1P2N4N2 atoms are approximately coplanar, the torsion angle being 2.2°. The Ni–N distances, of average 2.059 Å, are comparable to the corresponding values in complexes **7** and **9**, and are within the normal range for a five-coordinate nickel complex. The P–N distances of average

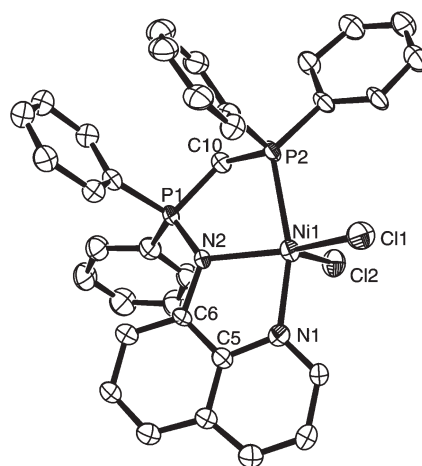


Fig. 5 ORTEP drawing of complex **11** (30% probability).

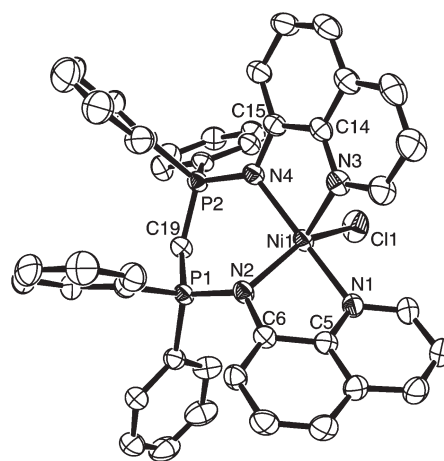


Fig. 6 ORTEP drawing of complex **13** (30% probability; toluene molecule is omitted). Selected bond lengths (Å) and angles (°): Ni(1)–N(1) 2.068(4), Ni(1)–N(2) 2.056(3), Ni(1)–N(3) 2.056(4), Ni(1)–N(4) 2.055(3), Ni(1)–Cl(1) 2.3115(13), P(1)–N(2) 1.625(3), P(1)–C(19) 1.713(4), P(2)–N(4) 1.611(4), P(2)–C(19) 1.691(4); N(4)–Ni(1)–N(3) 79.73(15), N(4)–Ni(1)–N(2) 97.27(14), N(3)–Ni(1)–N(2) 115.41(15), N(4)–Ni(1)–N(1) 170.52(14), N(3)–Ni(1)–N(1) 93.63(15), N(2)–Ni(1)–N(1) 79.37(14), N(4)–Ni(1)–Cl(1) 94.73(10), N(3)–Ni(1)–Cl(1) 100.62(11), N(2)–Ni(1)–Cl(1) 143.46(12), N(1)–Ni(1)–Cl(1) 93.14(11), P(1)–N(2)–Ni(1) 119.10(18), P(2)–N(4)–Ni(1) 121.3(2), N(2)–P(1)–C(19) 111.23(19), N(4)–P(2)–C(19) 108.8(2), P(1)–C(19)–P(2) 126.4(3).

1.618 Å show that the P–N bond has a bond order significantly greater than unity.²¹ The P–C19 distances of average 1.702 Å are in between that of a formal single (1.83 Å) and double (1.57 Å) bonds.²¹

Catalytic studies of the nickel complexes

(1) Cross-coupling of aryl chlorides with arylzinc reagents.

In our previous studies of the cross-coupling of organozinc reagents using an amido pincer nickel as the catalyst a 1 : 1 mixture of THF and NMP was found to be the most suitable solvent.¹¹ Hence we first examined the catalysis of complexes **2a**, **4**, **7**, **9**, **11** and **13** towards the cross-coupling of *p*-MeOC₆H₄Cl with *p*-MeC₆H₄ZnCl in a 1 : 1 mixture of THF and NMP. The results showed that the yields are **7** > **4**, **11** > **9**, **2a** > **13** (entries 1–6, Table 1). The low catalytic activity of complex **13** may result from a overcrowded coordination environment which prevents interaction between the central nickel atom and the reaction substrates. However, the activity difference of the other complexes seems to arise from electronic effects. Complexes **7** and **9** have very similar skeleton structures. The stronger electron donor ability of pyridyl group than imino group results in higher catalytic activity of the former. The Ph₂P group is also a stronger electron donor group than the imino group, and hence complex **11** is more active than complex **9**. In complex **4** the phenyl anion binds and transfers its electrons to the central metal ion and hence leads to an increase of electron density of the nickel. Indeed, complex **4** exhibits good catalytic activity. Bidentate coordinated complexes seem to be less effective than tridentate coordinated complexes for this series of studied complexes.

We also tested the reaction in THF or NMP (entries 7 and 8, Table 1) and the results showed that both of these solvents are less effective than a 1 : 1 mixture of THF and NMP. It was also noted that the **7**-catalyzed cross-coupling can be further improved by increasing the catalyst loadings, 2 mol% of **7** leading to 80% product yield and 4 mol% of **7** giving 91% product yield (entries 9 and 10, Table 1).

With the optimized reaction conditions, we tested reactions between functionalized phenyl chlorides and various arylzinc chlorides catalyzed by **7**. Because the functional groups are electron-withdrawing ones which activate the C–Cl bonds, the

Table 1 Evaluation of complexes **2a**, **4**, **7**, **9**, **11** and **13** in catalytic cross-coupling of *p*-MeOC₆H₄Cl with *p*-MeC₆H₄ZnCl^a

Entry	Cat. (mol%)	Solvent	Yield ^b (%)
1	2a (1)	NMP–THF (1 : 1)	36
2	4 (1)	NMP–THF (1 : 1)	50
3	7 (1)	NMP–THF (1 : 1)	76
4	9 (1)	NMP–THF (1 : 1)	38
5	11 (1)	NMP–THF (1 : 1)	50
6	13 (1)	NMP–THF (1 : 1)	Trace
7	7 (1)	THF	69
8	7 (1)	NMP	71
9	7 (2)	NMP–THF (1 : 1)	80
10	7 (4)	NMP–THF (1 : 1)	91

^a Reactions were performed with 0.5 mmol *p*-MeOC₆H₄Cl and 0.75 mmol *p*-MeC₆H₄ZnCl at 80 °C for 12 h. ^b Isolated product yield.

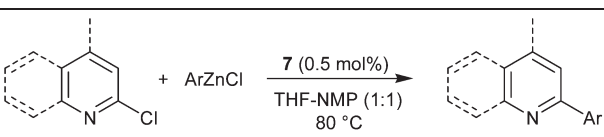
reactions require only 0.5 mol% catalyst loadings. Each of reactions of *p*-MeC₆H₄ZnCl with the phenyl chlorides bearing *p*-benzoyl, *p*-ethoxyformyl and *p*-aminoformyl groups gives almost quantitative cross-coupling product in 2 or 3 h, whereas (2-chlorophenyl)(phenyl)methanone displays lower reactivity due to steric hindrance of the *o*-benzoyl group; its reaction with *p*-MeC₆H₄ZnCl requires a period of 24 h to reach completion, giving the cross-coupling product in 91% yield. Reaction of *o*-MeC₆H₄ZnCl with *p*-ClC₆H₄C(O)Ph, *p*-ClC₆H₄COOEt, and *p*-ClC₆H₄C(O)NEt₂ gives comparable results to those of *p*-MeC₆H₄ZnCl. The electron-rich arylzinc reagents including *p*-MeOC₆H₄ZnCl, *p*-Me₂NC₆H₄ZnCl and 2-furylzinc chloride also displayed excellent reactivity in the catalytic reaction. Their reactions with *p*-ClC₆H₄C(O)Ph and *p*-ClC₆H₄COOEt lead to excellent results. Reactions of electron-deficient arylzinc reagent, *p*-CF₃C₆H₄ZnCl, with *p*-ClC₆H₄C(O)Ph and *p*-ClC₆H₄COOEt, respectively, under the same conditions as those mentioned above also afford the corresponding products in high yields, but longer reaction time is necessary. It should be indicated that the reactions using *p*-MeOC₆H₄ZnCl and *p*-CF₃C₆H₄ZnCl as the nucleophiles require 2.5 equiv. of zinc reagents due to homo-coupling of the arylzinc reagents (Table 2).

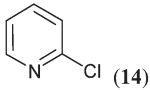
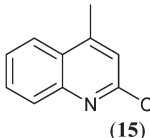
Complex **7** catalyzes the cross-coupling of heteroaryl chlorides and arylzinc chlorides under the same conditions as indicated above and the screened results are listed in Table 3. Reaction of *p*-MeC₆H₄ZnCl with either 2-chloropyridine or 2-chloro-4-methylquinoline gives almost quantitative yield in 6 h (entries 1 and 2, Table 3). *o*-MeC₆H₄ZnCl shows a little lower reactivity. Its reaction with 2-chloropyridine requires a longer reaction time and gives the desired product in 84% yield while reaction of *o*-MeC₆H₄ZnCl with 2-chloro-4-methylquinoline requires 1 mol% catalyst loading and 24 h reaction time (entries 3 and 4, Table 3). Reactions of *p*-CF₃C₆H₄ZnCl as an electron-deficient nucleophile with 2-chloropyridine and 2-chloro-4-methylquinoline, respectively, result in good product yields in

Table 2 Complex **7**-catalyzed cross-coupling of aryl chlorides with arylzinc chlorides^a

Entry	R	Ar	t/h	Yield ^b (%)
1	<i>p</i> -PhC(O)	<i>p</i> -MeC ₆ H ₄	2	99
2	<i>p</i> -COOEt	<i>p</i> -MeC ₆ H ₄	3	96
3	<i>p</i> -C(O)NEt ₂	<i>p</i> -MeC ₆ H ₄	3	99
4	<i>o</i> -PhC(O)	<i>p</i> -MeC ₆ H ₄	24	91
5	<i>p</i> -PhC(O)	<i>o</i> -MeC ₆ H ₄	4	98
6	<i>p</i> -C(O)NEt ₂	<i>o</i> -MeC ₆ H ₄	9	99
7	<i>p</i> -COOEt	<i>o</i> -MeC ₆ H ₄	4	95
8 ^c	<i>p</i> -COOEt	<i>p</i> -CH ₃ OC ₆ H ₄	3	96
9	<i>p</i> -PhC(O)	<i>p</i> -Me ₂ NC ₆ H ₄	5	94
10	<i>p</i> -PhC(O)	2-Furyl	1.5	99
11 ^c	<i>p</i> -COOEt	<i>p</i> -CF ₃ C ₆ H ₄	12	92
12 ^c	<i>p</i> -PhC(O)	<i>p</i> -CF ₃ C ₆ H ₄	9	90

^a Unless otherwise stated reactions were performed with 0.5 mmol aryl chlorides and 0.75 mmol arylzinc chlorides according to the conditions indicated by the above equation. ^b Isolated product yield. ^c 2.5 equiv. of arylzinc reagents were employed, NMP–THF = 1.5 : 2.5.

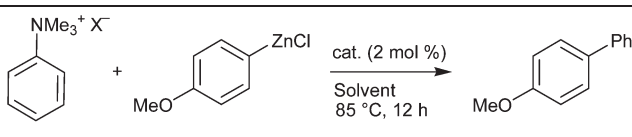
Table 3 Complex **7**-catalyzed cross-coupling of heteroaryl chlorides with arylzinc chlorides^a


Entry	Aryl chloride	Ar	t/h	Yield ^b (%)
1		<i>p</i> -MeC ₆ H ₄	6	99
2		<i>p</i> -MeC ₆ H ₄	6	99
3	14	<i>o</i> -MeC ₆ H ₄	24	84
4 ^c	15	<i>o</i> -MeC ₆ H ₄	24	99
5 ^d	14	<i>p</i> -CF ₃ C ₆ H ₄	12	84
6 ^d	15	<i>p</i> -CF ₃ C ₆ H ₄	12	90
7 ^d	14	<i>p</i> -CH ₃ OC ₆ H ₄	0.5	99
8 ^d	15	<i>p</i> -CH ₃ OC ₆ H ₄	1	95
9	14	<i>p</i> -Me ₂ NC ₆ H ₄	1	99
10	15	<i>p</i> -Me ₂ NC ₆ H ₄	1	92
11	14	2-Furyl	2	87
12	15	2-Furyl	2	96

^a Unless otherwise stated reactions were performed with 0.5 mmol aryl chlorides and 0.75 mmol arylzinc reagents according to the conditions indicated by the above equation. ^b Isolated product yield. ^c 1 mol% cat. was employed. ^d 2.5 equiv. of arylzinc chlorides were employed, NMP-THF = 1.5 : 2.5.

12 h although the yields are a little lower than those using *p*-MeC₆H₄ZnCl as a nucleophile (entries 5 and 6, Table 3). Electron-rich nucleophiles such as *p*-MeOC₆H₄ZnCl, *p*-Me₂NC₆H₄ZnCl and 2-furylzinc chloride are highly reactive. Their reactions with either 2-chloropyridine or 2-chloro-4-methylquinoline afford the corresponding cross-coupling products in excellent yields in 0.5–2 h (entries 7–12, Table 3). In the reactions using heteroaryl chlorides as the electrophiles 2.5 equiv. of *p*-MeOC₆H₄ZnCl or *p*-CF₃C₆H₄ZnCl were employed, which is the same situation as those of reactions employing substituted phenyl chlorides as the electrophilic substrates.

(2) Cross-coupling of aryltrimethylammonium salts with arylzinc chlorides. Encouraged by the good results in the reaction of arylzincs with aryl or heteroaryl chlorides catalyzed by the complexes mentioned above, we further tested catalysis of the complexes in the reaction of aryltrimethylammonium salts with arylzinc reagents. The catalytic activity of the complexes was first evaluated using reaction of PhNMe₃⁺I⁻ with *p*-MeOC₆H₄ZnCl in a 1 : 1 mixture of NMP and THF and the results are listed in Table 4 (entries 1–6). Complex **7** gave the highest product yield compared with **2a**, **4**, **9**, **11** and **13**. However, surprisingly, 1 equiv. of LiBr additive results in higher product yield when catalyzed with **7** under the same conditions (entry 7, Table 4). This experimental fact impelled us to examine the counterion effect. The results show that bromide is the most

Table 4 Screening of catalysts, counterions and solvents^a


Entry	Catalyst	X	Solvent	Yield ^b (%)
1	2a	I	THF-NMP (1 : 1)	33
2	4	I	THF-NMP (1 : 1)	50
3	7	I	THF-NMP (1 : 1)	85
4	9	I	THF-NMP (1 : 1)	56
5	11	I	THF-NMP (1 : 1)	60
6	13	I	THF-NMP (1 : 1)	Trace
7	7	I	THF-NMP (1 : 1)	92 ^c
8	7	Br	THF-NMP (1 : 1)	98
9	7	Cl	THF-NMP (1 : 1)	95
10	7	BF ₄	THF-NMP (1 : 1)	65
11	7	OTf	THF-NMP (1 : 1)	75
12	7	Br	THF	11
13	7	Br	NMP	80
14	7	Br	Tol.-NMP (1 : 1)	84

^a The reactions were carried out with 0.5 mmol PhNMe₃⁺X⁻ and 0.75 mmol *p*-MeOC₆H₄ZnCl according to the conditions indicated by the above equation unless otherwise stated. ^b Isolated product yields. ^c 1 equiv. of LiBr was added.

reactive electrophile in comparison with the electrophiles with I⁻, Cl⁻, BF₄⁻ and OTf⁻ as the counterions. Chloride has a close reactivity to the bromide and the BF₄ salt is the least reactive (entries 8–11, Table 4). This may result from interaction of the central metal with the anions during the catalytic cycle. Thus, the halogen anions may enter the catalytic process through coordination to the central nickel which stabilizes the central metal and tunes the electron density distributions around the central metal. Weakly coordinating OTf⁻ and non-coordinating anion BF₄⁻ do not provide or provide less stabilizing and tuning actions.²⁵ We also examined other solvents and found that each of THF, NMP and the 1 : 1 mixture of toluene and NMP is less effective than the 1 : 1 mixture of THF and NMP (entries 12–14, Table 4).

Next we tested the **7**-catalyzed reaction of activated, unactivated and deactivated aryltrimethylammonium bromides with arylzincs under the optimized conditions and the results are presented in Table 5. Besides *p*-MeOC₆H₄ZnCl listed in Table 4, both *p*-MeC₆H₄ZnCl and *p*-Me₂NC₆H₄ZnCl also react smoothly with PhNMe₃⁺Br⁻ in the presence of 1 mol% **7**, giving cross-coupling products in 90 and 98% yields, respectively (entries 1 and 2, Table 5). However, reaction of *o*-MeC₆H₄ZnCl with PhNMe₃⁺Br⁻ leads to low product yield (entry 3, Table 5). This is ascribed to a steric hindrance effect of the *ortho*-methyl group of *o*-MeC₆H₄ZnCl. *p*-MeOC₆H₄NMe₃⁺Br⁻ shows lower reactivity compared with PhNMe₃⁺Br⁻. Its reaction with *p*-MeC₆H₄ZnCl in the presence of 2 mol% of **7** generates the desired product in 81% yield. Increasing the catalyst loading to 4 mol% results in 96% product yield (entries 4 and 5, Table 5). Reaction of the electron-rich nucleophile, *p*-Me₂NC₆H₄ZnCl, with *p*-MeOC₆H₄NMe₃⁺Br⁻ gives an excellent yield when 3 mol% of complex **7** is employed, while reaction of the electron-deficient nucleophile, *p*-CF₃C₆H₄ZnCl with *p*-MeOC₆H₄NMe₃⁺Br⁻ requires

Table 5 Complex **7**-catalyzed cross-coupling of aryltrimethylammonium bromides with arylzinc chlorides^a

Entry	R	Ar	Cat. 7 (mol%)	Yield ^b (%)
1	H	<i>p</i> -MeC ₆ H ₄	1	90
2	H	<i>p</i> -Me ₂ NC ₆ H ₄	1	98
3	H	<i>o</i> -MeC ₆ H ₄	1	46
4	MeO	<i>p</i> -MeC ₆ H ₄	2	81
5	MeO	<i>p</i> -MeC ₆ H ₄	4	96
6	MeO	<i>p</i> -Me ₂ NC ₆ H ₄	3	98
7	MeO	<i>p</i> -CF ₃ C ₆ H ₄	5	83
8	MeO	2-Furyl	3	65
9	COOEt	<i>p</i> -MeC ₆ H ₄	2	80
10	COOEt	<i>p</i> -Me ₂ NC ₆ H ₄	1	87
11	COOEt	<i>p</i> -MeOC ₆ H ₄	3	98
12	COOEt	<i>p</i> -CF ₃ C ₆ H ₄	4	88
13	COOEt	<i>o</i> -MeC ₆ H ₄	1	47
14	COOEt	<i>o</i> -MeC ₆ H ₄	4	48
15	COOEt	2-Furyl	3	97

^a The reactions were carried out with 0.5 mmol ArNMe₃⁺X⁻ and 0.75 mmol ArZnCl according to the conditions indicated by the above equation. ^b Isolated product yields.

higher catalyst loading (5 mol%) and results in lower product yield (83%) (entries 6 and 7, Table 5). 2-Furylzinc chloride also reacts with *p*-MeOC₆H₄NMe₃⁺Br⁻ in the presence of **7**, but the reaction leads to relatively low product yield (65%) (entry 8, Table 5). Increasing catalyst loading and lengthening the reaction time can not improve the reaction. *p*-EtO₂CC₆H₄NMe₃⁺Br⁻ reacts smoothly with electron-rich nucleophiles such as *p*-MeC₆H₄ZnCl, *p*-MeOC₆H₄ZnCl and *p*-Me₂NC₆H₄ZnCl, and electron-deficient nucleophile *p*-CF₃C₆H₄ZnCl, giving corresponding cross-coupling products in good to excellent yields (entries 9–12, Table 5). However, reaction of *p*-EtO₂CC₆H₄NMe₃⁺Br⁻ with *o*-MeC₆H₄ZnCl affords a poor result due to steric hindrance of the *ortho*-methyl group of *o*-MeC₆H₄ZnCl. Increasing catalyst loading can not improve the yield (entries 13 and 14, Table 5). Reaction of 2-furylzinc chloride with *p*-EtO₂CC₆H₄NMe₃⁺Br⁻ leads to an excellent result, 3 mol% catalyst loading giving 97% product yield.

Conclusions

We have synthesized and characterized a series of quinoline-based ligands and their lithium and nickel complexes. The reactivity and transformation of the complexes were studied. The catalysis of the nickel complexes toward the reactions of arylzinc reagents with aryl chlorides and aryltrimethylammonium salts were evaluated and the *N,N,N*-chelate nickel complex, [NiCl₂-{2-PyCH₂P(Ph₂)=N(8-C₉H₆N)}] (**7**), was found to be the most effective catalyst for the cross-coupling reactions. The catalytic reaction of arylzinc chlorides with aryl chlorides require only low catalyst loadings and tolerate a range of functional groups such as PhC(O), COOEt, C(O)NEt₂ and CF₃ groups. Both heteroaryl chlorides, including 2-chloropyridine and 2-chloro-4-methylquinoline, and 2-furylzinc chloride are applicable as

electrophilic or nucleophilic substrates for the cross-coupling. The catalysts can also be applied to the cross-coupling of activated, unactivated and deactivated aryltrimethylammonium salts with substituted arylzinc chlorides and 2-furylzinc chloride. The higher activity of complex **7** than the other complexes is ascribed to stronger electron donor ability of the ligand, whereas the low activity of complex **13** may be due to a crowded coordination environment.

Experimental

All experiments were performed under nitrogen using standard Schlenk and vacuum-line techniques. Solvents were distilled under nitrogen over sodium (toluene), sodium–benzophenone (benzene, THF, Et₂O and *n*-hexane), or CaH₂ (CH₂Cl₂) and degassed prior to use. NMP was dried with activated molecular sieves, distilled under reduced pressure and degassed. CDCl₃ and C₆D₆ were purchased from Cambridge Isotope Laboratories, Inc., degassed and stored over activated molecular sieves (CDCl₃) or Na/K alloy (C₆D₆). DMSO-*d*₆ was purchased from ARMAR Chemicals and used as received. LiBuⁿ, Ph₂PCl, (Ph₂P)₂CH₂, *p*-EtO₂CC₆H₄NMe₂, MeOTf and Me₃O⁺BF₄⁻ were purchased from Acros Organics and used as received. PhNMe₃⁺Cl⁻ and PhNMe₃⁺Br⁻ were purchased from TCI and used as received. PhNMe₂ was purchased from China National Medicines Corporation Ltd. and purified by distillation under reduced pressure prior to use. RNHPPH₂ (R = *p*-MeC₆H₄, Bu^t),²⁶ 8-azidoquinoline,²⁷ *p*-MeOC₆H₄NMe₂,²⁸ aryltrimethylammonium salts,^{16a} and ligands **6**,²⁹ **8**,²⁹ and **10**²⁷ were prepared according to the literature. ArZnCl were prepared *in situ* through reaction of ZnCl₂ with the corresponding aryllithium (*p*-MeC₆H₄Li,³⁰ *o*-MeC₆H₄Li,³⁰ *p*-Me₂NC₆H₄Li,³¹ *p*-CF₃C₆H₄Li,³² *p*-MeOC₆H₄Li³³ and 2-furyllithium³⁴). All other chemicals were obtained from commercial vendors and used as received. NMR spectra were recorded on a Bruker av300 spectrometer at ambient temperature. The chemical shifts of ¹H and ¹³C{¹H} NMR spectra are referenced to internal solvent resonances or TMS, and the ³¹P{¹H} NMR spectra are referenced to external 85% H₃PO₄. Infrared spectra were recorded on a Bruker VECTOR-22 spectrometer. Elemental analyses were performed by the Analytical Center of University of Science and Technology of China.

Syntheses

***p*-MeC₆H₄NHP(Ph₂)=N(8-C₉H₆N) (1a).** A three-necked flask was charged with 8-azidoquinoline (4.08 g, 24 mol) and CH₂Cl₂ (20 cm³) and to the solution was added dropwise a solution of *p*-MeC₆H₄NHPPH₂ (5.83 g, 20 mmol) in CH₂Cl₂ (15 cm³) with stirring. The resultant mixture was stirred for 4 h at room temperature. The solution was concentrated and then hexane was added. The resultant solution was kept at –20 °C to form yellow–brown crystals of **1a** (7.81 g, 90%). Anal. Calc. for C₂₈H₂₄N₃P·0.2C₆H₁₄: C, 77.81; H, 5.99; N, 9.32. Found: C, 78.00; H, 6.00; N, 9.37%. ¹H NMR (CDCl₃), δ 2.16 (s, 1H, CH₃), 6.83 (d, *J* = 7.8 Hz, 2H, Ar), 6.95 (d, *J* = 7.5 Hz, 2H, Ar), 7.19–7.29 (m, 2H, Ar), 7.37–7.53 (m, 6H, Ar), 7.54 (d, *J* = 6.6 Hz, 1H, Ar), 7.98–8.09 (m, 4H, Ar), 8.10 (d, *J* = 8.1 Hz, 1H,

Ar), 8.82 (s, 1H, Ar). ^{13}C NMR (CDCl_3): δ 38.47, 114.29, 119.88, 121.29, 121.68, 127.21, 127.29, 127.37, 127.97, 129.43, 129.55, 130.70, 130.76, 130.82, 130.88, 131.93, 132.07, 135.51, 143.22, 144.43, 148.16, 149.90. ^{31}P NMR (CDCl_3): δ 7.52.

BuⁿNHP(Ph)₂=N(8-C₉H₆N) (1b). A three-necked flask was charged with 8-azidoquinoline (4.08 g, 24 mmol) and CH_2Cl_2 (20 cm^3) and to the solution was added dropwise a solution of BuⁿNHPPPh₂ (5.15 g, 20 mmol) in CH_2Cl_2 (15 cm^3) with stirring. The resultant mixture was stirred for 4 h at room temperature. The solution was concentrated and then hexane was added. The resultant solution was kept at -20 °C to form red crystals of **1b** (7.35 g, 92%). Anal. Calc. for $\text{C}_{25}\text{H}_{26}\text{N}_3\text{P}$: C, 75.17; H, 6.56; N, 10.52. Found: C, 75.33; H, 6.65; N, 10.37%. ^1H NMR (CDCl_3): δ 1.01 (s, 9H, Buⁿ), 3.71 (d, $J = 5.4$ Hz, 1H, NH), 7.04–7.11 (m, 2H, Ar), 7.29–7.36 (m, 6H, Ar), 7.39–7.50 (m, 2H, Ar), 7.97 (dd, $J = 1.2, 8.4$ Hz, 1H, Ar), 8.01–8.09 (m, 4H, Ar), 8.17–8.22 (m, 1H, Ar). ^{13}C NMR (CDCl_3): δ 32.40, 115.05, 120.19, 121.75, 122.08, 123.29, 128.06, 128.23, 128.32, 128.37, 130.14, 131.77, 131.88, 136.18, 144.51. ^{31}P NMR (CDCl_3): δ -1.51.

[NiCl₂{N(8-C₉H₆N)=P(Ph)₂NH(*p*-MeC₆H₄)}] (2a). A Schlenk tube was charged with **1a** (0.867 g, 2 mmol), (DME)NiCl₂ (0.44 g, 2 mmol) and THF (30 cm^3) and the mixture was stirred at room temperature for 12 h. Solvent was removed and the residue was dissolved in CH_2Cl_2 and the resulting solution was filtered. The filtrate was concentrated *in vacuo* and a few drops of toluene were added to generate dark brown crystals of **2a** (0.94 g, 83%). Anal. Calc. for $\text{C}_{28}\text{H}_{24}\text{N}_3\text{Cl}_2\text{NiP}\cdot 0.4\text{C}_7\text{H}_8$: C, 61.82; H, 4.59; N, 7.03. Found: C, 61.66; H, 4.57; N, 7.22%. IR (KBr dispersion disc): ν (cm^{-1}) 3222s (NH), 1285vs (P=N).

A concentrated CH_2Cl_2 solution of **2a** was set aside for a few days to form single crystals used for X-ray diffraction analysis.

[NiCl₂{(1,2-C₆H₄)P(Ph)(NHBuⁿ)=N(8-C₉H₆N)}] (4). A Schlenk tube was charged with **1b** (0.799 g, 2 mmol), (DME)NiCl₂ (0.44 g, 2 mmol) and THF (30 cm^3) and the mixture was stirred at room temperature for 12 h. NaH (0.1 g, 60%, 2.5 mmol) was added and the resulting mixture was heated at 65–70 °C (bath temperature) for 24 h. The solution was cooled to room temperature and solvent was removed *in vacuo*. The residue was dissolved in CH_2Cl_2 and the resulting solution was filtered. The filtrate was concentrated *in vacuo* and then added hexane to form deep red crystals of **4** (0.601 g, 61%). Anal. Calc. for $\text{C}_{25}\text{H}_{25}\text{N}_3\text{ClNiP}\cdot 0.17\text{CH}_2\text{Cl}_2$: C, 59.62; H, 5.04; N, 8.29. Found: C, 59.61; H, 5.21; N, 8.05%. ^1H NMR (CDCl_3): δ 1.36 (s, 9H, Buⁿ), 3.19 (d, $J = 7.8$ Hz, 1H, NH), 6.84 (d, $J = 7.2$ Hz, 1H, Ar), 6.99–7.21 (m, 5H, Ar), 7.39–7.59 (m, 4H, Ar), 7.88–7.98 (m, 3H, Ar), 8.15 (d, $J = 8.4$ Hz, 1H, Ar), 9.19 (d, $J = 5.1$ Hz, 1H, Ar). ^{13}C NMR (CDCl_3): δ 32.07 (d, $J = 2.8$ Hz), 54.61 (d, $J = 1.8$ Hz), 115.03, 115.12, 116.18, 122.06, 124.44, 124.60, 127.46, 128.45, 128.68, 129.65, 129.77, 130.21, 131.17 (d, $J = 7.2$ Hz), 133.10, 137.32, 140.65 (d, $J = 13.7$ Hz), 147.05, 149.56. ^{31}P NMR (CDCl_3): δ 37.85. IR (KBr dispersion disc): ν (cm^{-1}) 3198s (NH), 1286m (P=N).

THF was added to a solution of **4** in CH_2Cl_2 which was then set aside to form single crystals used for X-ray diffraction analysis.

[Li{(1,2-C₆H₄)P(Ph)(NHBuⁿ)=N(8-C₉H₆N)}] (5). A solution of **1b** (0.352 g, 0.881 mmol) in THF (10 cm^3) was cooled to about -80 °C and to the solution was added dropwise a solution of LiBuⁿ (0.36 cm^3 , 2.5 M in hexanes, 0.9 mmol) with stirring. The resulting mixture was allowed to warm to room temperature and stirred overnight. Volatiles were removed *in vacuo*. The residue was dissolved in hexane and filtered. The filtrate was concentrated to afford yellow crystals of **5** (0.28 g, 78%). Anal. Calc. for $\text{C}_{25}\text{H}_{25}\text{N}_3\text{LiP}$: C, 74.07; H, 6.22; N, 10.37. Found: C, 74.20; H, 6.45; N, 10.11%. ^1H NMR (C_6D_6): δ 0.72 (s, 9H, Buⁿ), 3.56 (d, $J = 6.3$ Hz, 1H, NH), 6.29–6.33 (m, 1H, Ar), 6.64–6.79 (m, 6H, Ar), 7.22–7.32 (m, 2H, Ar), 7.64 (s, 1H, Ar), 7.72 (d, $J = 7.8$ Hz, 1H, Ar), 7.95 (dd, $J = 7.8, 10.8$ Hz, 4H, Ar). ^{13}C NMR (C_6D_6): δ 32.37, 52.97, 115.39, 120.12, 122.92, 123.29, 128.15, 129.02, 130.08 (d, $J = 2.2$ Hz), 132.10 (d, $J = 8.3$ Hz), 136.38, 144.17. ^{31}P NMR (C_6D_6): δ -2.93.

[NiCl₂{2-PyCH₂P(Ph)₂=N(8-C₉H₆N)}] (7). A mixture of **6** (0.839 g, 2 mmol), (DME)NiCl₂ (0.44 g, 2 mmol) and CH_2Cl_2 (30 cm^3) was stirred at room temperature for 5 h. The resulting solution was filtered and the filtrate was concentrated to yield yellow green crystals of complex **7** (0.89 g, 81%). Anal. Calc. for $\text{C}_{27}\text{H}_{22}\text{N}_3\text{Cl}_2\text{NiP}\cdot 0.06\text{CH}_2\text{Cl}_2$: C, 58.65; H, 4.02; N, 7.58. Found: C, 58.67; H, 4.14; N, 7.26%. IR (KBr dispersion disc): ν (cm^{-1}) 1282s (P=N).

A dilute solution of **7** in CH_2Cl_2 was set aside for a few days to form single crystals used for X-ray diffraction analysis.

[NiCl₂{N(Ph)=C(Ph)CH₂P(Ph)₂=N(8-C₉H₆N)}] (9). A mixture of **8** (1.18 g, 2.26 mmol), (DME)NiCl₂ (0.55 g, 2.5 mmol) and CH_2Cl_2 (30 cm^3) was stirred at room temperature for 12 h. The resulting solution was filtered and the filtrate was concentrated to yield red–orange crystals of complex **9** (1.12 g, 76%). Anal. Calc. for $\text{C}_{35}\text{H}_{28}\text{N}_3\text{Cl}_2\text{NiP}$: C, 64.56; H, 4.33; N, 6.45. Found: C, 64.79; H, 4.65; N, 6.40%. IR (KBr dispersion disc): ν (cm^{-1}) 1280vs (P=N).

THF was added to a solution of **9** in CH_2Cl_2 which was then set aside to form single crystals used for X-ray diffraction analysis.

[NiCl₂{P(Ph)₂CH₂P(Ph)₂=N(8-C₉H₆N)}] (11). A mixture of **10** (1.053 g, 2 mmol), (DME)NiCl₂ (0.44 g, 2 mmol) and THF (30 cm^3) was stirred at room temperature for 12 h. Volatiles were removed *in vacuo* and the residue was dissolved in CH_2Cl_2 . The resulting solution was filtered and the filtrate was concentrated to produce yellow–brown crystals of complex **11** (0.97 g, 74%). Anal. Calc. for $\text{C}_{34}\text{H}_{28}\text{N}_2\text{Cl}_2\text{NiP}_2$: C, 62.24; H, 4.30; N, 4.27. Found: C, 62.22; H, 4.24; N, 4.11%. IR (KBr dispersion disc): ν (cm^{-1}) 1280s (P=N).

A dilute solution of **11** in CH_2Cl_2 was set aside for a few days to form single crystals used for X-ray diffraction analysis.

[(8-C₉H₆N)N=P(Ph)₂]₂CH₂ (12). To a stirred solution of 8-azidoquinoline (8.17 g, 48 mmol) in CH_2Cl_2 (20 cm^3) was added dropwise a solution of dppm (7.69 g, 20 mmol) in CH_2Cl_2 (40 cm^3) at room temperature. The mixture was stirred for 8 h. Solvent was removed by rotary evaporation. The residual solid was washed with Et_2O and dried *in vacuo* to give a yellow orange powder of **12** (11.1 g, 83%). Anal. Calc. for $\text{C}_{43}\text{H}_{34}\text{N}_4\text{P}_2$: C, 77.23; H, 5.12; N, 8.38. Found: C, 76.93; H, 5.22; N, 8.17%.

^1H NMR (CDCl_3): δ 4.83 (t, $J = 13.8$ Hz, 2H, CH_2), 6.84–6.98 (m, 15H, Ar), 7.10 (d, $J = 6.9$ Hz, 2H, Ar), 7.20 (t, $J = 7.2$ Hz, 2H, Ar), 7.33 (t, $J = 6.5$ Hz, 1H, Ar), 7.43–7.51 (m, 1H, Ar), 7.53–7.65 (m, 7H, Ar), 7.73 (d, $J = 8.1$ Hz, 2H, Ar), 8.05 (d, $J = 2.7$ Hz, 2H, Ar). ^{13}C NMR (CDCl_3): δ 20.73, 114.02, 114.16, 119.08, 123.42 (d, $J = 18$ Hz), 127.70, 128.63, 128.96 (d, $J = 12.9$ Hz), 129.50, 131.78 (d, $J = 2.2$ Hz), 132.01 (d, $J = 9.5$ Hz), 132.33, 132.75, 136.52, 148.02. ^{31}P NMR (CDCl_3): δ 8.04.

[NiCl $\{$ (8-C $_9$ H $_6$ N)NP(Ph $_2$) $\}_2$ CH] (13). To a stirred solution of **12** (1.31 g, 1.96 mmol) in THF (30 cm 3) was added dropwise a solution of LiBu n (0.8 cm 3 , 2.5 M in hexanes, 2 mmol) at about -80 °C. The resulting mixture was warmed to room temperature and stirred for 4 h. This solution was then transferred into a suspension of (DME)NiCl $_2$ (0.44 g, 2 mmol) in THF (10 cm 3) at about -80 °C. The mixture was warmed to room temperature and stirred for 12 h. Volatiles were removed *in vacuo* and the residue was dissolved in CH $_2$ Cl $_2$. The resulting solution was filtered and the filtrate was concentrated. Hexane was added to form red crystals of complex **13** (0.975 g, 61%). Anal. Calc. for C $_{43}$ H $_{33}$ N $_4$ ClNiP $_2$ ·0.6CH $_2$ Cl $_2$: C, 64.43; H, 4.24; N, 6.89. Found: C, 64.31; H, 4.31; N, 6.98%. IR (KBr dispersion disc): ν (cm $^{-1}$) 1276s (P=N).

Toluene was added to a solution of **13** in CH $_2$ Cl $_2$ which was then set aside to form single crystals used for X-ray diffraction analysis.

***p*-EtO $_2$ CC $_6$ H $_4$ NMe $_3^+$ Br $^-$.** To a stirred solution of ethyl 4-dimethylaminobenzoate (1.20 g, 6.2 mmol) in DMF (10 cm 3) was added dropwise an excess of methyl bromide at room temperature. The resulting solution was stirred for 4 days. Solvent was removed *in vacuo*. The residue was washed with Et $_2$ O (10 cm 3 \times 3) and dried under vacuum to give a white solid (1.75 g, 98%). Anal. Calc. for C $_{12}$ H $_{18}$ BrNO $_2$: C, 50.01; H, 6.30; N, 4.86. Found: C, 49.87; H, 6.29; N, 4.76%. ^1H NMR (DMSO- d_6): δ 1.34 (t, $J = 7.2$ Hz, 3H, Et), 3.66 (s, 9H, NMe), 4.51 (q, $J = 7.2$ Hz, 2H, Et), 8.15 (s, 4H, C $_6$ H $_4$). ^{13}C NMR (DMSO- d_6): δ 14.03, 56.33, 61.33, 121.43, 130.56, 131.21, 150.48, 164.33.

***p*-MeOC $_6$ H $_4$ NMe $_3^+$ Br $^-$.** To a stirred solution of 4-methoxy-*N*,*N*-dimethylbenzenamine (0.52 g, 3.4 mmol) in DMF (8 cm 3) was added dropwise an excess of methyl bromide at room temperature. The resulting solution was stirred for 56 h. Solvent was removed *in vacuo* and the residue was washed with Et $_2$ O (10 cm 3 \times 3), dried under vacuum to give a white solid (0.77 g, 92%). Anal. Calc. for C $_{10}$ H $_{16}$ BrNO: C, 48.80; H, 6.55; N, 5.69. Found: C, 48.90; H, 6.52; N, 5.71%. ^1H NMR (DMSO- d_6): δ 3.60 (s, 3H, OMe), 3.82 (s, 9H, NMe), 7.12 (d, $J = 9.6$ Hz, 2H, C $_6$ H $_4$), 7.91 (d, $J = 9.6$ Hz, 2H, C $_6$ H $_4$). ^{13}C NMR (DMSO- d_6): δ 55.77, 56.57, 114.66, 121.86, 140.10, 159.59.

X-Ray crystallography

Single crystals of complexes **2a**, **4**, **7**, **9**, **11** and **13** were respectively mounted in Lindemann capillaries under nitrogen. Diffraction data were collected on a Bruker Smart CCD area-detector with graphite-monochromated Mo-K α radiation ($\lambda = 0.71073$ Å)

(for complexes **2a**, **4**, **9**, **11** and **13**) or an Oxford Diffraction Gemini S Ultra diffractometer with mirror-monochromated Cu-K α radiation ($\lambda = 1.54184$ Å) (for complex **7**). The structures were solved by direct methods using SHELXS-97 35 and refined against F^2 by full-matrix least squares using SHELXL-97. 36 The disordered solvent molecule in complex **7** was removed from the diffraction data using the SQUEEZE program. Examination of the structure of complex **11** with PLATON showed that there is a potential solvent-accessible void in the crystal lattice. This may result from molecule stacking since no definitive solvent molecule could be found. The data were modified using the SQUEEZE program. Hydrogen atoms were placed at calculated positions. Crystal data and experimental details of the structure determinations are listed in Table 6.

Catalytic cross-coupling of aryl chlorides with arylzinc chlorides

A typical procedure is exemplified by the reaction of *p*-CH $_3$ OC $_6$ H $_4$ Cl with *p*-CH $_3$ C $_6$ H $_4$ ZnCl using complex **7** as a catalyst. A Schlenk tube was charged with *p*-CH $_3$ OC $_6$ H $_4$ Cl (0.0713 g, 0.5 mmol), NMP (1.5 cm 3) and complex **7** (0.0114 g, 0.02 mmol). To the stirred mixture a solution of *p*-CH $_3$ C $_6$ H $_4$ ZnCl (1.5 cm 3 , a 0.5 M solution in THF, 0.75 mmol) was added by syringe. Then the reaction mixture was stirred at 80 °C (bath temperature) for 24 h. The solution was cooled to room temperature. Water (10 cm 3) and several drops of hydrochloric acid were successively added. The resulting mixture was extracted with Et $_2$ O (10 cm 3 \times 3). The combined extract was dried (MgSO $_4$) and concentrated to dryness. The residue was purified by column chromatography (silica gel, eluted using petroleum ether) to afford a white solid (0.0902 g, 91%).

Catalytic cross-coupling of aryltrimethylammonium salts with arylzinc chlorides

A typical procedure is exemplified by the reaction of PhNMe $_3^+$ Br $^-$ with *p*-CH $_3$ OC $_6$ H $_4$ ZnCl using complex **7** as a catalyst. PhNMe $_3^+$ Br $^-$ (0.108 g, 0.5 mmol), complex **7** (0.0057 g, 0.01 mmol) and NMP (1.5 cm 3) were added to a Schlenk tube. To the stirred mixture was added a solution of *p*-CH $_3$ OC $_6$ H $_4$ ZnCl (1.5 cm 3 , a 0.5 M solution in THF, 0.75 mmol) by syringe. The reaction mixture was stirred at 85 °C (bath temperature) for 12 h and then cooled to room temperature. Water (10 cm 3) and several drops of acetic acid were successively added. The resulting mixture was extracted with Et $_2$ O (10 cm 3 \times 3). The extract was dried (Na $_2$ SO $_4$) and concentrated. The residue was purified by column chromatography (silica gel, eluted using petroleum ether) to afford a white solid (0.0903 g, 98%).

Acknowledgements

This research was supported by National Basic Research Program of China (grant no. 2009CB825300) and the National Natural Science Foundation of China (grant no. 20772119). The authors thank Professors D.-Q. Wang and S.-M. Zhou for determining the crystal structures. We also thank Professor G.-P. Yong for helpful discussion on crystal structures.

Table 6 Details of the X-ray structure determinations of complexes **2a**, **4**, **7**, **9**, **11** and **13**

	2a ·0.5CH ₂ Cl ₂	4 ·THF	7	9 ·CH ₂ Cl ₂ ·THF	11	13 ·1.5C ₇ H ₈
Empirical formula	C ₂₉ H ₂₆ Cl ₄ N ₃ NiP	C ₂₉ H ₃₃ ClN ₃ NiOP	C ₂₇ H ₂₂ Cl ₂ N ₃ NiP	C ₄₀ H ₃₈ Cl ₄ N ₃ NiOP	C ₃₄ H ₂₈ Cl ₂ N ₂ NiP ₂	C ₁₀₇ H ₉₀ Cl ₂ N ₈ Ni ₂ P ₄
<i>M_r</i>	648.01	564.71	549.06	808.21	656.13	1800.07
<i>T/K</i>	298(2)	298(2)	291(2)	298(2)	298(2)	298(2)
Crystal system	Monoclinic	Triclinic	Monoclinic	Triclinic	Orthorhombic	Triclinic
Space group	<i>P</i> 2 ₁ / <i>n</i>	<i>P</i> $\bar{1}$	<i>C</i> 2/ <i>c</i>	<i>P</i> $\bar{1}$	<i>P</i> 2 ₁ 2 ₁ 2 ₁	<i>P</i> $\bar{1}$
<i>a</i> /Å	12.1681(11)	10.1230(10)	34.5863(13)	11.4343(15)	14.7449(16)	11.7609(14)
<i>b</i> /Å	16.3886(15)	11.83510(12)	11.5292(2)	11.6020(15)	13.6940(14)	12.4767(16)
<i>c</i> /Å	14.9929(13)	12.17190(13)	19.6821(5)	17.1801(19)	16.1341(19)	17.3590(18)
α /°	90	99.2830(10)	90	76.682(2)	90	82.3720(10)
β /°	94.7500(10)	111.966(2)	117.126(4)	73.1970(10)	90	85.171(2)
γ /°	90	92.9710(10)	90	64.5420(10)	90	79.2300(10)
<i>V</i> /Å ³	2979.6(5)	1324.64(13)	6985.0(3)	1955.1(4)	3257.7(6)	2475.6(5)
<i>Z</i>	4	2	8	2	4	2
<i>D_c</i> /g cm ⁻³	1.445	1.416	1.044	1.373	1.338	1.207
<i>F</i> (000)	1328	592	2256	836	1352	938
μ /mm ⁻¹	1.087	0.922	2.758	0.846	0.883	0.549
θ range/°	2.42–25.01	1.76–25.01	2.87–62.76	2.20–25.02	2.76–25.02	1.67–25.02
No. reflns collected	15 435	7006	13 149	10 204	15 728	13 056
No. indep. reflns	5256	4591	5522	6709	5668	8566
<i>R</i> _{int}	0.0826	0.0297	0.0354	0.0646	0.1945	0.0239
No. data/restraints/params	5256/0/372	4591/0/359	5522/0/307	6709/0/507	5668/0/370	8566/0/632
Goodness of fit on <i>F</i> ²	1.062	1.022	1.015	1.309	1.050	1.001
Final <i>R</i> indices ^a [<i>I</i> > 2 σ (<i>I</i>)]	<i>R</i> ₁ = 0.0532, <i>wR</i> ₂ = 0.1108	<i>R</i> ₁ = 0.0435, <i>wR</i> ₂ = 0.0623	<i>R</i> ₁ = 0.0378, <i>wR</i> ₂ = 0.1095	<i>R</i> ₁ = 0.0858, <i>wR</i> ₂ = 0.1953	<i>R</i> ₁ = 0.0984, <i>wR</i> ₂ = 0.1595	<i>R</i> ₁ = 0.0569, <i>wR</i> ₂ = 0.1716
<i>R</i> indices (all data)	<i>R</i> ₁ = 0.1066, <i>wR</i> ₂ = 0.1249	<i>R</i> ₁ = 0.0833, <i>wR</i> ₂ = 0.0686	<i>R</i> ₁ = 0.0453, <i>wR</i> ₂ = 0.1125	<i>R</i> ₁ = 0.1415, <i>wR</i> ₂ = 0.2113	<i>R</i> ₁ = 0.2389, <i>wR</i> ₂ = 0.1844	<i>R</i> ₁ = 0.0945, <i>wR</i> ₂ = 0.1936
$\Delta\rho_{\max, \min}$ /e Å ⁻³	0.398, -0.605	0.333, -0.289	0.265, -0.208	0.920, -0.751	0.641, -0.686	0.718, -0.407

$$^a R_1 = \frac{\sum ||F_o| - |F_c||}{\sum |F_o|}; wR_2 = \left[\frac{\sum w(F_o^2 - F_c^2)^2}{\sum w(F_o^4)} \right]^{1/2}$$

Notes and references

- (a) *Metal-Catalyzed Cross-Coupling Reactions*, ed. F. Diederich and P. J. Stang, VCH, Weinheim, 1998; (b) *Metal-Catalyzed Cross-Coupling Reactions*, ed. A. de Meijere and F. Diederich, Wiley-VCH, Weinheim, 2nd edn, 2004; (c) *Transition Metal Reagents and Catalysts: Innovations in Organic Synthesis*, ed. J. Tsuji, John Wiley & Sons, Chichester, 2000; (d) *Cross-coupling Reactions: A Practical Guide*, ed. N. Miyaura, Springer, Berlin, 2002.
- (a) J. Hassan, M. Sévignon, C. Gozzi, E. Schulz and M. Lemaire, *Chem. Rev.*, 2002, **102**, 1359; (b) J.-P. Corbet and G. Mignani, *Chem. Rev.*, 2006, **106**, 2651; (c) A. C. Frisch and M. Beller, *Angew. Chem., Int. Ed.*, 2005, **44**, 674; (d) K. C. Nicolaou, P. G. Bulger and D. Sarlah, *Angew. Chem., Int. Ed.*, 2005, **44**, 4442; (e) G. Manolikakes and P. Knochel, *Angew. Chem., Int. Ed.*, 2009, **48**, 205; (f) S. Würtz and F. Glorius, *Acc. Chem. Res.*, 2008, **41**, 1523; (g) G. C. Fu, *Acc. Chem. Res.*, 2008, **41**, 1555.
- (a) M. R. Netherton and G. C. Fu, *Adv. Synth. Catal.*, 2004, **346**, 1525; (b) A. F. Littke and G. C. Fu, *Angew. Chem., Int. Ed.*, 2002, **41**, 4176; (c) *Organozinc Reagents, A Practical Approach*, ed. P. Knochel and P. Jones, Oxford University Press, New York, 1999; (d) *The Chemistry of Organozinc Compounds*, ed. Z. Rappoport and I. Marek, John Wiley & Sons, Chichester, 2006; (e) V. B. Phapale and D. J. Cárdenas, *Chem. Soc. Rev.*, 2009, **38**, 1598; (f) E. Negishi, Z. Huang, G. Wang, S. Mohan, C. Wang and H. Hattori, *Acc. Chem. Res.*, 2008, **41**, 1474; (g) E. Negishi, Q. Hu, Z. Huang, M. Qian and G. Wang, *Aldrichimica Acta*, 2005, **38**, 71.
- (a) T. R. Hoye and M. Chen, *J. Org. Chem.*, 1996, **61**, 7940; (b) S. Marquis and M. Arlt, *Tetrahedron Lett.*, 1996, **37**, 5491; (c) E. G. Corley, K. Conrad, J. A. Murry, C. Savarin, J. Holko and G. Boice, *J. Org. Chem.*, 2009, **69**, 5120; (d) M. Okano, M. Amano and K. Takagi, *Tetrahedron Lett.*, 1998, **39**, 3001; (e) K. Krascensicsova, P. Walla, P. Kasak, G. Uray, C. O. Kappe and M. Putala, *Chem. Commun.*, 2004, 2606; (f) Z. Huang, M. Qian, D. J. Babinski and E. Negishi, *Organometallics*, 2005, **24**, 475; (g) I. Kondoloff, H. Doucet and M. Santelli, *Organometallics*, 2006, **25**, 5219; (h) J. M. Herbert, *Tetrahedron Lett.*, 2004, **45**, 817; (i) A. Alimardanov, L. Schmieder-van de Vondervoort, A. H. M. de Vries and J. G. de Vries, *Adv. Synth. Catal.*, 2004, **346**, 1812; (j) I. Sapountzis, H. Dube and P. Knochel, *Adv. Synth. Catal.*, 2004, **346**, 709.
- (a) C. Dai and G. C. Fu, *J. Am. Chem. Soc.*, 2001, **123**, 2719; (b) J. Huang and S. P. Nolan, *J. Am. Chem. Soc.*, 1999, **121**, 9889, and references therein.
- W. A. Herrmann, V. P. W. Bohm and C.-P. Reisinger, *J. Organomet. Chem.*, 1999, **576**, 23.
- J. E. Milne and S. L. Buchwald, *J. Am. Chem. Soc.*, 2004, **126**, 13028.
- (a) S. Calimsiz, M. Sayah, D. Mallik and M. G. Organ, *Angew. Chem., Int. Ed.*, 2010, **49**, 2014; (b) M. G. Organ, S. Avola, I. Dubovyk, N. Hadei, E. A. B. Kantchev, C. J. O'Brien and C. Valente, *Chem.-Eur. J.*, 2006, **12**, 4749.
- (a) B. H. Lipshutz, B. A. Frieman, C.-T. Lee, A. Lower, D. M. Nihan and B. R. Taft, *Chem.-Asian J.*, 2006, **1**, 417; (b) B. H. Lipshutz and P. A. Blomgren, *J. Am. Chem. Soc.*, 1999, **121**, 5819; (c) J. A. Miller and R. P. Farrell, *Tetrahedron Lett.*, 1998, **39**, 6441; (d) C. E. Tucker and J. G. de Vries, *Top. Catal.*, 2002, **19**, 111; (e) Z. Xi, Y. Zhou and W. Chen, *J. Org. Chem.*, 2008, **73**, 8497; (f) S. Son and G. C. Fu, *J. Am. Chem. Soc.*, 2008, **130**, 2756.
- (a) H.-U. Blaser, A. Indolese, F. Naud, U. Nettekoven and A. Schnyder, *Adv. Synth. Catal.*, 2004, **346**, 1583; (b) P. Walla and C. O. Kappe, *Chem. Commun.*, 2004, 564; (c) A. Gavryushin, C. Kofink, G. Manolikakes and P. Knochel, *Org. Lett.*, 2005, **7**, 4871; (d) A. Gavryushin, C. Kofink, G. Manolikakes and P. Knochel, *Tetrahedron*, 2006, **62**, 7521.
- (a) L. Wang and Z.-X. Wang, *Org. Lett.*, 2007, **9**, 4335; (b) C. Zhang and Z.-X. Wang, *Organometallics*, 2009, **28**, 6507; (c) N. Liu, L. Wang and Z.-X. Wang, *Chem. Commun.*, 2011, **47**, 1598.
- S. Ueno, N. Chatani and F. Kakiuchi, *J. Am. Chem. Soc.*, 2007, **129**, 6098.
- E. Wenkert, A.-L. Han and C.-J. Jenny, *J. Chem. Soc., Chem. Commun.*, 1988, 975.
- J. T. Reeves, D. R. Fandrick, Z. Tan, J. J. Song, H. Lee, N. K. Yee and C. H. Senanayake, *Org. Lett.*, 2010, **12**, 4388.
- S. B. Blakey and D. W. C. MacMillan, *J. Am. Chem. Soc.*, 2003, **125**, 6046.
- (a) L.-G. Xie and Z.-X. Wang, *Angew. Chem., Int. Ed.*, 2011, **50**, 4901; (b) X.-Q. Zhang and Z.-X. Wang, *J. Org. Chem.*, 2012, **77**, 3658.

- 17 (a) X. Cui, J. Li, Z.-P. Zhang, Y. Fu, L. Liu and Q.-X. Guo, *J. Org. Chem.*, 2007, **72**, 9342; (b) P. Evans, P. Hogg, R. Grigg, M. Nurmabi, J. Hinsley, V. Sridharan, S. Suganthan, S. Korn, S. Collard and J. E. Muir, *Tetrahedron*, 2005, **61**, 9696; (c) A. Scrivanti, M. Bertoldini, U. Matteoli, S. Antonaroli and B. Crociani, *Tetrahedron*, 2009, **65**, 7611; (d) K. Komura, H. Nakamura and Y. Sugi, *J. Mol. Catal. A: Chem.*, 2008, **293**, 72.
- 18 A. Buchard, R. H. Platel, A. Auffrant, X. F. Le Goff, P. Le Floch and C. K. Williams, *Organometallics*, 2010, **29**, 2892.
- 19 A. Hashimoto, H. Yamaguchi, T. Suzuki, K. Kashiwabara, M. Kojima and H. D. Takagi, *Eur. J. Inorg. Chem.*, 2010, 39.
- 20 L. Wang, C. Zhang and Z.-X. Wang, *Eur. J. Inorg. Chem.*, 2007, 2477.
- 21 (a) D. E. C. Corbridge, *Phosphorus*, Elsevier, Amsterdam, 1985, p. 38; (b) P. Imhoff, R. van Asselt, C. J. Elsevier, K. Vrieze, K. Goubitz, K. F. van Malssen and C. H. Stam, *Phosphorus, Sulfur Silicon Relat. Elem.*, 1990, **47**, 401.
- 22 K. Sun, L. Wang and Z.-X. Wang, *Organometallics*, 2008, **27**, 5649.
- 23 (a) M. Stol, D. J. M. Snelders, M. D. Godbole, R. W. A. Havenith, D. Haddleton, G. Clarkson, M. Lutz, A. L. Spek, G. P. M. van Klink and G. van Koten, *Organometallics*, 2007, **26**, 3985; (b) M. Shen, P. Hao and W.-H. Sun, *J. Organomet. Chem.*, 2008, **693**, 1683; (c) Z.-X. Wang and Z.-Y. Chai, *Eur. J. Inorg. Chem.*, 2007, 4492.
- 24 T. Koga, H. Furutachi, T. Nakamura, N. Fukita, M. Ohba, K. Takahashi and H. Okawa, *Inorg. Chem.*, 1998, **37**, 989.
- 25 A. Zapf and M. Beller, *Chem.–Eur. J.*, 2001, **7**, 2908.
- 26 (a) S. Kato, M. Goto, R. Hattori, K. Nishiwaki, M. Mizuta and M. Ishida, *Chem. Ber.*, 1985, **118**, 1668; (b) H. R. Sisler and N. L. Smith, *J. Org. Chem.*, 1961, **26**, 611.
- 27 A. Saravanamuthu, D. M. Ho, M. E. Kerr, C. Fitzgerald, M. R. M. Bruce and A. E. Bruce, *Inorg. Chem.*, 1993, **32**, 2202.
- 28 L. Huang, X. Zhang and Y. Zhang, *Org. Lett.*, 2009, **11**, 3730.
- 29 W.-A. Ma and Z.-X. Wang, *Organometallics*, 2011, **30**, 4364.
- 30 H. Gilman, E. A. Zoellner and W. M. Selby, *J. Am. Chem. Soc.*, 1933, **55**, 1252.
- 31 B. Bernard, J. Marc and R.-M. Miguel, *Synthesis*, 1980, **11**, 926.
- 32 R. Pereira, A. Furst, B. Iglesias, P. Germain, H. Gronemeyer and A. R. de Lera, *Org. Biomol. Chem.*, 2006, **4**, 4514.
- 33 L. Jin, J. Xin, Z. Huang, J. He and A. Lei, *J. Am. Chem. Soc.*, 2010, **132**, 9607.
- 34 B. J. Wakefield, *Organolithium Methods*, Academic Press, London, 1988.
- 35 G. M. Sheldrick, *Acta Crystallogr., Sect. A: Found. Crystallogr.*, 1990, **46**, 467.
- 36 G. M. Sheldrick, *SHELXL97, Programs for structure refinement*, Universität Göttingen, 1997.